

Design and Analysis of Armour-Piercing Fin-Stabilized Discarding Sabot

¹Quratulain, ²Badar Rashid, ³Asim Shehzad, ⁴Arshad Mehmood, ²Umair Saleem, ¹Muhammad Atif Niaz

Abstract—An Armour-Piercing Fin-Stabilized Discarding Sabot (APFSDS) is highly energetic and ballistic ammunition used for piercing armored vehicles and battle tanks. These ballistic rounds impart high kinetic energy to the target that involves high strain rates and melting temperatures. The lethality of ammunition is tested against RHA depth it would penetrate. This paper discusses the terminal ballistic aspect of the penetrator and presents the study of design parameters for an APFSDS to achieve optimal penetration. The trend of penetration depths across the range of length-to-diameter ratios is presented. A tungsten alloy APFSDS is tested against Rolled Homogenous Armour (RHA) via FEA simulations. A simplified penetrator model is created and parameterized in Design Modeler. Explicit dynamics numerical schemes are used. Johnson-Cook strength and failure models are chosen along with Mie-Grüneisen state of equation model. ANSYS Autodyn solver is used for simulating the impact.

Keywords - APFSDS; Penetrator; Rolled Homogenous Armour; Tungsten Alloy; Explicit Dynamics; Johnson-Cook; Mie-Grüneisen; ANSYS; Simulations

I. INTRODUCTION

Kinetic energy penetrators (KEPs) are ammunitions that penetrate through an armoured vehicle by inflicting local damage to the targeted area. They do not hold any explosives and they cause the damage mainly by the kinetic energy imparted into the target. These penetrators have high strength and density which facilitate their penetrating capability. These projectiles are also effective against composites and ceramics. The slender and rod-like geometry of Armour-Piercing Fin-Stabilized Discarding Sabot (APFSDS) provides the necessary profile required to cause local damage while high velocities of up to Mach number 4 – 6 provide the desired kinetic energy. The impact of these projectiles is tested against benchmark materials like Rolled Homogenous Armour (RHA).

With the increase in armor protection level, extensive research is being done in the areas of increasing aspect ratio of penetrator along with velocity and mass consideration [1]. APFSDS being slender unlike other tank rounds require centralization within the barrel. Sabots are used to overcome this issue, moreover, they also ensure that the propellant gases do not leak for complete transfer of the propulsive force to the

kinetic energy of the projectile. Modern antiarmor kinetic energy projectiles are being designed with high length to diameter ratio (L/D), with fins and sabots for stability from tumbling in flight and optimum conversion of propulsive energy to kinetic energy respectively.

The muzzle velocity should be high for maximum kinetic energy. Doing so, ammunition will need large forces to accelerate in the bore. It demands a larger diameter to achieve maximum acceleration from the propellant. This is contrary to the requirement of a small diameter required for large penetration. To deal with this problem we install a lightweight structure i.e. the sabots which increase the effective diameter inside the bore and discard as soon as it leaves the barrel to have less dissipation of kinetic energy during ammunition flight [2].

An APFSDS goes through four stages of ballistics dynamics.

- Internal Ballistics
- Intermediate Ballistics
- External Ballistics
- Terminal Ballistics

The stage associated with the impact and penetration is the final stage i.e., when the penetrator hits the RHA target. The parameters that are discussed here also govern the performance of terminal ballistics.

II. SUITABLE MODELS AND MATERIAL PROPERTIES

Comparing with internal, intermediate and external ballistics, theory of terminal ballistics is relatively new. Impact on solid plates has been studied using the analytical, experimental, and numerical methods. Although discretization methods have proved to be powerful and versatile analysis tools [3,4]. However, Due to the complicated nature of the impact process, the scope of theoretical analysis has been in general very limited. Recently, experimental techniques have become very sophisticated, but an extensive study of the impact process would quickly overwhelm available resources [5].

The numerical simulations provide a promising approach, as compared to experimental investigation in terms of cost effectiveness and safe alternatives to the development of warheads, kinetic energy penetrators and armours. Moreover, the numerical simulations when combined with judicious use of experimentation can provide valuable insight into complex weapon/target interactions. Shock wave propagation through materials, high-rate material behaviours, and material failure

Manuscript received 28th September 2020 Accepted 30th October 2020.

¹ Wah Engineering College, University of Wah, Wah Cantt, Pakistan

² National University of Technology, Islamabad, Pakistan

³ Institute of Space Technology Islamabad, Pakistan

University of Engineering and Technology, Jalozi Campus Peshawar

Corresponding Author: tariqasim@yahoo.com

are all essential characteristics of such interactions that cannot be captured in a well-controlled, documented fashion as done in numerical simulations.

In this research, a parametric study to assess the influence of existing Johnson-Cook constitutive model parameters on the simulation of tungsten rods penetrating rolled homogeneous armour (RHA) steel targets is successfully performed. Mie-Grüneisen model is also used to capture the shock wave propagation through the medium. One of the initial goals of the effort is to identify a “best possible” combination of tungsten and RHA model parameters to use for simulations across a wide range of conditions of interest to the development of KE penetrators. The study will consider tungsten rods with different length-to diameter (L/D) ratios against fixed striking velocity 1600 m/s.

Parameterization and CAD model are discussed in section III. Whereas, section IV of the paper provides a detailed discussion on the Methodology used during the work. Conclusion of the work presented in this paper is penned down in section V.

A. Explicit Integration Scheme

Dynamic material behaviour is different from that of quasi-static response, which is carried out in a stepwise manner and the number of intermediate steps tends to infinity thus system equilibrium is maintained [6]. Contrary to this the material does not have enough time to physically react to deform in dynamic material behaviour with the decreased duration of event. This results in high local stresses and high local deformations at the location of contact-impact. The explicit integration method is capable of capturing this short time structural response through a number of smaller time steps sufficient enough to capture the complete behaviour of the structure under an impact phenomenon. This is mainly because it uses direct solvers to solve the set of equations at each time step and takes less computational time compared to that of implicit solvers. [7]

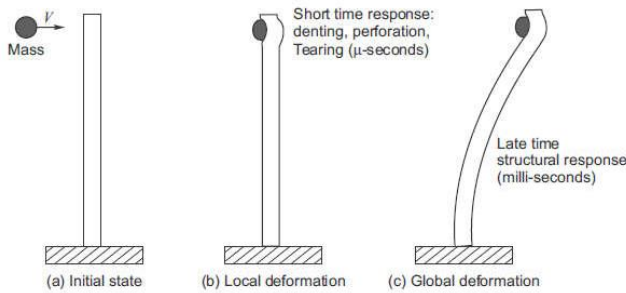


Fig 1: Local and global response of a bar [6]

Explicit dynamics or explicit integration schemes are extensively used for impact. The deformation of materials on impact is not a linear process. The non-linearity of these materials, in fact, ensures the authenticity of results and why penetrators penetrate a material when the material is subjected to high temperatures and stresses. The strain rates applicable for the impact process are on the order of 10^3 .

Explicit dynamics being a time-based integration method is used to simulate these non-linear and inelastic deformation

processes. An APFSDS penetration with an impact velocity of more than 1000 m/s has a very high strain rate. It can be clearly seen in Fig 1 that why an explicit-dynamic integration-based method is necessary as the damage is local.

Unlike implicit methods, explicit dynamics do not have the problem of convergence. To simulate the impact of an APFSDS, AUTODYN is used with appropriate material properties and flow-stress models.

B. Johnson-Cook Strength Model

The Johnson-Cook constitutive model describes the flow stress (σ) of a metal as a function of plastic strain (ϵ_p), plastic strain rate ($\dot{\epsilon}_p$), and temperature (T), as given in equation 1 to 3.

$$\sigma_y = (A + B\bar{\epsilon}_p^n)(1 + C\ln(\dot{\epsilon}^*)) (1 - (T^*)^m) \quad (1)$$

$$\dot{\epsilon}^* = \frac{\dot{\epsilon}_p}{\dot{\epsilon}_0} \quad (2)$$

$$T^* = \frac{T - T_r}{T_m - T_r} \quad (3)$$

In this model

A, B, C, n and m	= Model parameters (constants)
T_{melt}	= Material melting temperature
T_{room}	= Ambient temperature
$\dot{\epsilon}_0$	= Reference plastic strain rate.

The model parameters are typically derived from material characterization experiments through a fitting process intended to reproduce the trends observed in the characterization experiments while minimizing error. [8]

C. Johnson-Cook Failure Model

The failure model relates the failure strain to material properties (D1 to D5 coefficients), tri-axiality stress, and temperature.

$$\epsilon_f = [D_1 + D_2 e^{D_3 \sigma^*}] [1 + D_4 \ln(\dot{\epsilon}_p^*)] [1 + D_5 T^*] \quad (5)$$

In equation 4,

D1 to D5	= Material constants
σ^*	= Stress tri-axiality ratio
σ_m	= Mean stress / hydrostatic stress[8]

D. Mie-Grüneisen Equation of State

The Mie-Grüneisen model relates the pressure, internal energy and the volume of a solid at a given temperature. It determines the pressure in a shock-compressed solid. The Mie-Grüneisen relation given in equation 5 describes the effect of changing volume of a crystal lattice on its vibrational properties.

$$p = p_H + \Gamma \rho (e - e_H) \quad (5)$$

Here,

Γ	= Grüneisen parameter, representing thermal pressure from a set of vibrating atoms.
p	= Pressure
e	= Internal energy
p_H	= Reference pressure

e_H = Internal energy

For dynamic experiments ' u_p ' and ' U ' in most solids and many liquids exhibit a linear relation as given in equation 6 [6].

$$U = c_0 + su_p \quad (6)$$

E. Material Properties

The material properties necessary for a Johnson-Cook (J-C) model for both Tungsten Alloy and RHA are presented in Table I and II, respectively. These properties are interpolated to match the experimental data and confirmed through the simulations in AUTODYN solver of Explicit Dynamics module (ANSYS Workbench).

TABLE I
TUNGSTEN ALLOY MODEL CO-EFFICIENT

Tungsten Alloy		
Parameters	Values	Units
Density	17700	Kg/m ³
Specific Heat	134	J/(Kg.K)
Initial Yield Stress	1.186 x 10 ⁹	Pa
Hardening Constant	1.05 x 10 ⁹	Pa
Hardening Exponent	0.6125	-
Strain Rate Constant	0.02247	-
Thermal Softening Exponent	1	-
Melting Temperature	1723	K
Shear Modulus	1.60 x 10 ¹¹	Pa
Grüneisen Coefficient	1.54	-
Parameter C1	4029	m/s
Parameter C2	1.237	-
Parameter Quadratic S2	0	s/m

TABLE II
RHA MODEL CO-EFFICIENT

Rolled Homogenous Armour		
Parameters	Value	Units
Density	7850	Kg/m ³
Yield Strength	1.185 x 10 ⁹	Pa
Reference Strain Rate	1	s ⁻¹
Grüneisen Coefficient	1.67	-
Damage Constant D1	0.05	-
Damage Constant D2	3.44	-
Damage Constant D3	-2.12	-
Damage Constant D4	0.002	-
Damage Constant D5	0.61	-
Parameter C1	4610	m/s
Parameter C2	1.73	-
Parameter Quadratic S2	0	s/m

III. PARAMETERIZATION & CAD MODEL

In the current study impact velocity of the penetrator is fixed at 1600 m/s with the target plate being 2 kilometers away from the firing position. The muzzle velocity and internal ballistics are also fixed therefore no variation in impact velocities is considered. Materials for the penetrator and target plate have already been chosen. They do not constitute the set of design parameters. Therefore, only variable parameters are geometry related. Length and diameter

influence penetration the most. A CAD model to represent the L/D ratio is created exclusively. The diameter and length are parameterized in Design Modeler (ANSYS) see Fig 2 & 3.



Fig 2: Penetrator geometry created in CATIA with windshield

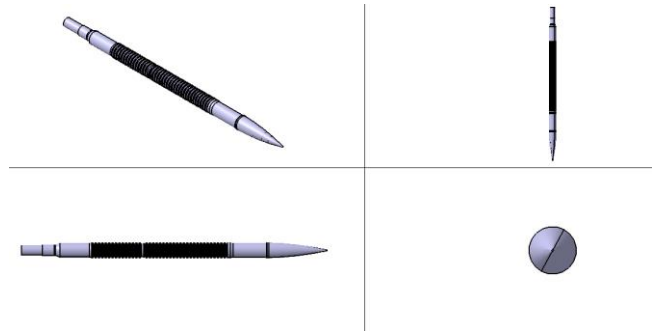


Fig 3: Isometric views of Penetrator

A. Simplification

According to the Lanz-Odermatt empirical models on penetration depths and L/D. The rod-like geometry of the penetrator contributes to penetration. The presence of windshield/tip serves the aerodynamics purpose of reducing drag [8]. The CAD model is, therefore, simplified into a rod of length 476 mm and diameter being 28 mm. This simplification makes the study easier by shifting the focus on L/D ratio. The computational process is also simplified with significant reduction in simulation time by considering a quarter of the penetrator and the target. The Fig 4 shows a quarter section of the whole model.

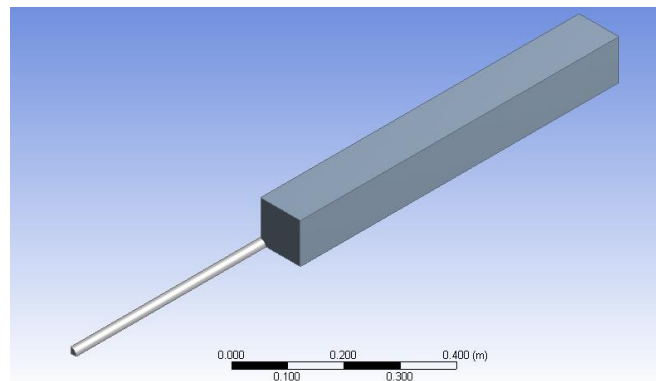


Figure 4: Penetrator and target geometry: isometric view (quarter sections)

B. Parameterization

To identify the optimal point, a refined sweep must be performed in a specified range. Different design points are considered for the parametric study of L/D with two cases. Case-I studies only the variation of diameter while case-II considers variable length with fixed diameter as shown in

Table-III and Fig 5.

Table of Design Points				
	A	B	C	D
1	Name	Update Order	P1 - RADIUS	P2 - Length
2	Units		m	m
3	DP 3	1	0.0119	0.476
4	DP 2	2	0.012526	0.476
5	DP 1	3	0.013222	0.476
6	DP 0	4	0.014	0.476
7	DP 4	5	0.014875	0.476
8	DP 5 (Current)	6	0.015866	0.476
9	DP 6	7	0.014	0.504
10	DP 7	8	0.014	0.448
11	DP 8	9	0.014	0.532
12	DP 9	10	0.014	560

Fig 5: Design points for parametric study (Case I)

TABLE III
L/D RATIOS FOR PARAMETRIC STUDY

Case-I	All dimensions are in mm		
	L/D	L	D
1	15	476	31.732
2	16	476	29.75
3	17	476	28
4	18	476	26.44
5	19	476	25.052
6	20	476	23.8
Case-II			
7	16	448	28
8	18	504	28
9	19	532	28
10	20	560	28

IV. METHODOLOGY

After the selection of mathematical models and considering the simplifications, the CAD models of target plate and penetrator were prepared in the Design Modeler license within the ANSYS Workbench. The length and diameter of the penetrator were parameterized to study the effects of varying L/D ratio on penetration length. After the CAD Modelling, the simulations were run to verify the material properties with the experimental data. A total number of 10 simulations as shown in Table III were run to acquire a data of the penetration lengths with respect to the yield strength of the target material i.e. Rolled Homogenous Armour (RHA). For these simulations a mesh element size of 8 mm was used so that lesser time was required to execute and finish the simulation.

Other than the material properties, certain necessary phenomenon like shear bending/ adiabatic shearing, “mushrooming” were also observed as shown in Fig 6 to verify that the Johnson-Cook Model predicts the phenomena as expected.

After verifying the material properties with the experimental data, the simulations for parameterized penetrator geometry were carried out with the L/D ratio varying from 15 to 20.

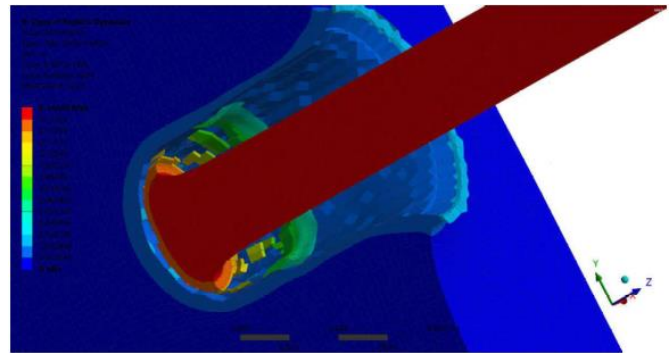


Fig 6: Mushrooming in half 3D simulation

Another empirically established observation is that the diameter of the opening on target face as shown in Fig 7. Approximately 100 microseconds for velocities greater than 1000 m/s is 2-3 times the maximum diameter of the penetrator.

$$D_{open} = 2.155 D_{penetrator} \tag{7}$$

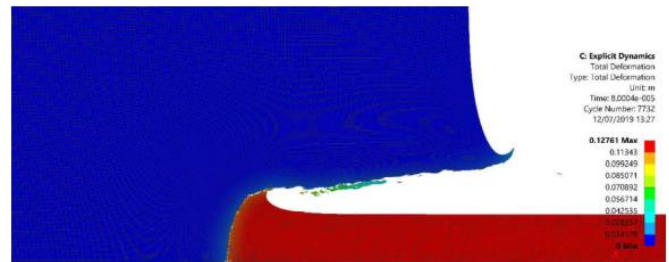


Fig 7: Front face of target plate showing opening cavity

V. RESULTS

The results with varying L/D from 15 to 20 for both the cases i.e., with constant diameter and constant are tabulated in Table IV.

TABLE IV
L/D RATIOS AND PENETRATION LENGTHS

Case-I	All dimensions are in mm			
	L/D	L	D	Penetration Length(s)
1	15	476	31.732	520
2	16	476	29.75	501
3	17	476	28	460
4	18	476	26.44	468
5	19	476	25.052	367
6	20	476	23.8	421
Case-II				
7	16	448	28	449
8	18	504	28	502
9	19	532	28	532
10	20	560	28	552

Fig 8 shows variation of penetration length as we are changing the penetrator diameter while keeping the penetrator length to 476 mm. This plot shows that there’s a limit to what extent the diameter of a penetrator can be decreased while keeping the length constant.

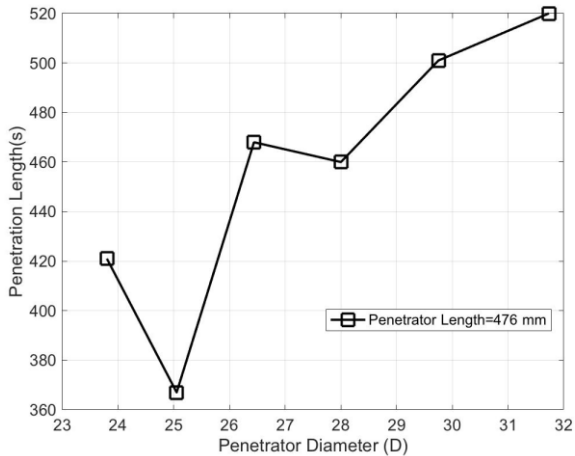


Fig 8: Penetration Length (P) vs. Penetrator Diameter (L)

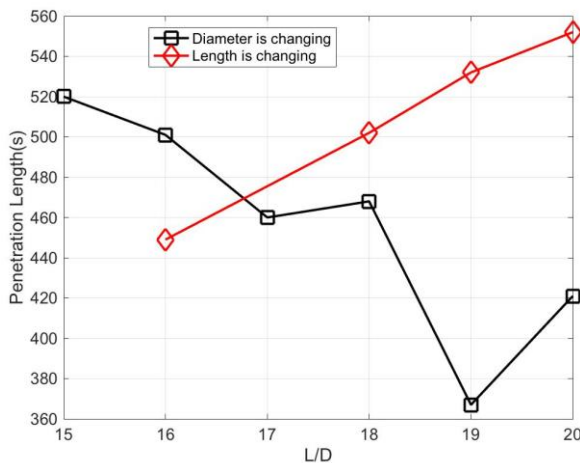


Fig 9: Penetration Length (P) vs. Length/Diameter (L/D)

Fig 9 shows variation of penetration length as a function of penetrator's length to diameter ratio. The penetration length for an L/D of more than 18 shows a reduction in the penetration length. This can be explained by a reduction in the mass and kinetic energy of the penetrator.

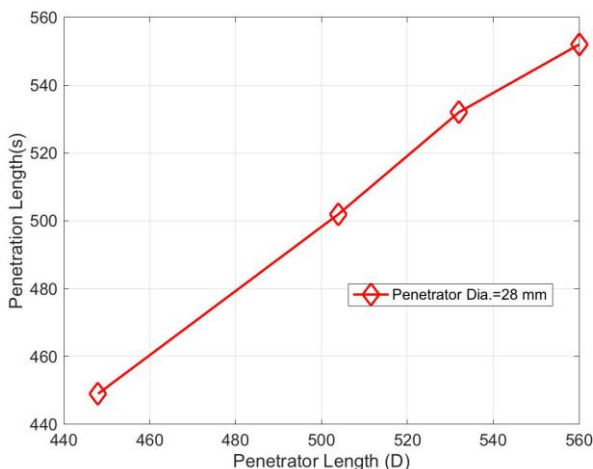


Figure 10: Penetration Length (P) vs. Penetrator Length (L)

Variation of penetration length as a function of penetrator length while keeping the penetrator diameter to 28 mm is shown in Fig 10. This plot shows that high stresses for a penetrator of smaller cross-sectional area also make the penetrator more vulnerable to damage.

VI. CONCLUSIONS

The Kinetic energy penetrators (KEPs) are ammunitions that penetrate through an armoured protection of the vehicle and inflicts local damage to the desired and targeted area. There are no explosives involved in this process thus damage caused here is mainly by the kinetic energy imparted into the target.

The penetrators have high strength and density facilitating the penetrating ability to these objects. The projectiles are very effective against different types of materials inclusive of composites and ceramics. The slender and rod-like geometry of these objects provide required profile to inflict local damage when high velocities such as Mach number 4 – 6 are used which generate desired kinetic energy into these objects.

In the current study, impact of these projectiles is tested against benchmark materials such as Rolled Homogenous Armour (RHA).

A numerical simulation to study the effects of varying L/D ratio on penetration length is performed in this work. In this regards penetrator's length and diameters in a specific range are varied to observe the outcome. It has been observed that there's a limit to what extent the diameter of a penetrator can be decreased while keeping the length constant.

It has also been observed that the penetration length for a value of L/D more than 18 shows a reduction in the penetration length. Moreover, it can also be observed that the high stresses for a penetrator of smaller cross-sectional area also make the penetrator more vulnerable to damage.

REFERENCES

- [1] Sorensen, B. R. (1991). Design and analysis of kinetic-energy projectiles using finite-element optimization. *Final report, 1 Jan-1 Jul 90 (No. AD-A-242988/4/XAB; BRL-TR--3289)*. Army Armament Research and Development Command, Aberdeen Proving Ground, MD (United States). Ballistics Research Lab.
- [2] Bulman, D. N., & Ferries, J. G. (2001). The Dynamic Modelling of a Novel Design of 120mm APFSDS Training Round. *Danby Engineering Ltd Yorkshire (United Kingdom)*.
- [3] Khan, Abid Ali ;Ming, Xu Yuan and Ming, Wang Xin (1997). Knowledge Representation in Case Based Reasoning for Finite Element Analysis. *2nd Asian Pacific Conference on Aerospace Technology and Science (APCAT '97) 6 - 10 October, Dun Huang Gansu, China*.
- [4] Khan, Abid Ali;Ahmed, Faiz;Memon, Iqbal Rasool and Ming, Xu Yuan. (2002) Error Computations for Adaptive Finite Element Analysis. *Journal of Engineering and Applied Sciences (JEAS)*, University of Engineering and Technology, Peshawar. Vol 21 No 2 pp 53 – 60.
- [5] Farrar, C. L., & Leeming, D. W. (1983). *Military ballistics: a basic manual*. Brassey's Publishers.
- [6] Mukhopadhyay, Debasis & Bhattacharyya, Kamal. (2009). Are all Quasi-static Processes Reversible?.
- [7] Zukas, J. (2004). Introduction to hydrocodes. Elsevier.

- [8] C. Lakshmana Rao, V. Narayanamurthy, K. R. Y. Simha, *Applied Impact Mechanics*, Wiley, 2016, pp.195-196.
- [9] Lanz, W., & Odermatt, W. (1992, June). Penetration limits of conventional large caliber antitank guns kinetic energy projectiles. *In Proc. of the 13th International Symposium on Ballistics*, Stockholm, Sweden.